Contribution from the Department of Chemistry,
Colorado State University, Fort Collins, Colorado 80523

Synthesis, Structures, and Electrochemistry of Copper(II)–Mercaptide Complexes

OREN P. ANDERSON,* CHRISTOPHER M. PERKINS, and KARREN K. BRITO

Received April 23, 1982

Copper(II) complexes of ligand **1**, the monoanion of 3,9-dimethyl-4,8-diazaundeca-3,8-diene-2,10-dione dioxime, have been shown to form stable copper(II)–mercaptide complexes with *p*-chlorothiophenol and thiophenol. Thus, the intensely green complexes [Cu(**1**)(*p*-ClC_6H_4S)] (**2**) and [Cu(**1**)(C_6H_5S)] (**3**) have been synthesized and characterized by visible spectroscopy, structure determination, and cyclic voltammetry. Both **2** and **3** exhibit two intense transitions (428 and 354 nm for **2**, 428 and 355 nm for **3**), which have been attributed to charge-transfer transitions. The structures of **2** and **3** are very similar, as both consist of neutral, monomeric square-pyramidal complexes in which mercaptide sulfur occupies the apical position (Cu–S = 2.424 (1) Å in both **2** and **3**). Complex **2** crystallized in $P2_1/c$, with a = 10.536 (2) Å, b = 12.793 (3) Å, c = 15.061 (3) Å, β = 105.50 (1)°, and Z = 4. Complex **3** crystallized in *Pbca*, with a = 13.072 (2) Å, b = 14.940 (2) Å, c = 18.786 (3) Å, and Z = 8. The structure of **2** was refined by least-squares methods to R = 0.041 and R_w = 0.040 for 2294 reflections, while for **3** R = 0.030 and R_w = 0.033 for 2572 reflections. Complexes **2** and **3** exhibit quasi-reversible reduction of the Cu(II)–mercaptide center at −0.85 V (vs. SCE), a value that is consistent with the charge-transfer assignment of the two prominent bands in the visible spectrum.

Introduction

The highly unusual spectroscopic properties[1] of the copper(II) centers in the type 1 "blue" copper proteins have never been duplicated in toto in any copper(II) complex of normal molecular weight. Spectroscopic and theoretical studies[2] have suggested that the spectroscopic properties manifested in the visible and EPR spectra for these proteins arise from the combination of a highly distorted tetrahedral coordination environment about the copper atom and the binding of a mercaptide sulfur atom to the metal. Both of these aspects of the coordination about copper(II) in type 1 sites have been confirmed by structural studies on the metalloproteins.[3-5]

The interest of coordination chemists in these intriguing natural systems has led to many attempts to create "models" for the type 1 copper sites by synthesizing complexes containing copper(II)–mercaptide linkages. This is a challenging synthetic problem, however, due to the facile redox reaction (eq 1) that

$$2\text{Cu(II)} + 2\text{RS}^- \rightarrow 2\text{Cu(I)} + \text{RS–SR} \qquad (1)$$

normally converts copper(II) and mercaptide sulfur to copper(I) and a disulfide. Thus, attempts at synthesis of Cu(II)–mercaptide complexes have generally resulted in unstable[6,7] and/or incompletely characterized[8-20] materials.

Two cases in which stable copper(II)–mercaptide bonds have been definitely established are known, however. In the first of these, uncertainty concerning the nature of the mixed-valence complexes[21] involving copper and thiol-bearing ligands such as penicillamine was resolved by the structural characterizations[22-24] of copper mixed-valence clusters. In these clusters, mercaptide sulfur was found to be coordinated to Cu(I) and Cu(II) simultaneously. The only noncluster copper(II)–mercaptide complex that has been structurally characterized is the green, paramagnetic adduct formed between the macrocyclic $[Cu(tet\ b)]^{2+}$ complex ion and the *o*-mercaptobenzoate dianion.[25] In that five-coordinate, neutral, monomeric complex, the mercaptide sulfur was found to occupy an equatorial site in the trigonal-bipyramidal coordination array about copper(II), at a distance of 2.359 (4) Å.

The paucity of compounds involving copper(II)–mercaptide coordination has led us to adopt the goal of synthesizing the widest possible variety of such complexes. Knowing the synthetic difficulties inherent in these systems (alluded to above), it was decided initially to design synthetic schemes that would give the maximum chances of isolating stable Cu(II)–S(mercaptide) complexes.

Our synthetic scheme is based on a mechanistic study[26] of the anaerobic oxidation of 2-mercaptosuccinic acid by copper(II). The mechanism suggested by this study was a nonradical process involving initial formation of a dimeric species containing two copper(II) ions bridged by mercaptide sulfur atoms. In the rate-determining step of this process, the actual

(1) (a) Malkin, R.; Malmström, B. G. *Adv. Enzymol. Relat. Areas Mol. Biol.* **1970**, *33*, 177. (b) Malmström, B. G.; Vanngård, T. *J. Mol. Biol.* **1960**, *2*, 118. (c) Malmström, B. G. *Pure Appl. Chem.* **1970**, *24*, 393. (d) Fee, J. A. *Struct. Bonding (Berlin)* **1975**, *23*, 1. (e) Gray, H. B. *Adv. Inorg. Biochem.* **1980**, *2*, 1. (f) Gray, H. B.; Solomon, E. I. In "Copper Proteins"; Spiro, T. G., Ed.; Wiley: New York, 1981; Vol. 3, Chapter 1.
(2) (a) Dooley, D. M.; Rawlings, J.; Dawson, J. H.; Stephens, P. J.; Andreasson, L.; Malmström, B. G.; Gray, H. B. *J. Am. Chem. Soc.* **1979**, *101*, 5038–5053. (b) Roberts, J. E.; Brown, T. G.; Hoffman, B. M.; Peisach, J. *Ibid.* **1980**, *102*, 825–829. (c) Solomon, E. I.; Hare, J. W.; Dooley, D. M.; Dawson, J. H.; Stephens, P. J.; Gray, H. B. *Ibid.* **1980**, *102*, 168–178.
(3) Colman, P. M.; Freeman, H. C.; Guss, J. M.; Murata, M.; Norris, V. A.; Ramshaw, J. A. M.; Venkatappa, M. P. *Nature (London)* **1978**, *272*, 319–324.
(4) Adman, E. T.; Stenkamp, R. E.; Sieker, L. C.; Jensen, L. H. *J. Mol. Biol.* **1978**, *123*, 35–47.
(5) Tullius, T. D.; Frank, P.; Hodgson, K. O. *Proc. Natl. Acad. Sci. U.S.A.* **1978**, *75*, 4069–4073.
(6) Thompson, J. S.; Marks, T. J.; Ibers, J. A. *Proc. Natl. Acad. Sci. U.S.A.* **1977**, *74*, 3114–3118.
(7) Thompson, J. S.; Marks, T. J.; Ibers, J. A. *J. Am. Chem. Soc.* **1979**, *101*, 4180.
(8) Amundsen, A. R.; Whelan, J.; Bosnich, B. *J. Am. Chem. Soc.* **1977**, *99*, 6730.
(9) Downes, J. M.; Whelan, J.; Bosnich, B. *Inorg. Chem.* **1981**, *20*, 1081–1086.
(10) Roewer, G.; Kuhne, K.; Kempe, G. *Z. Chem.* **1976**, *16*, 117.
(11) Braithwaite, A. C.; Rickard, C. E. F.; Waters, T. N. *Transition Met. Chem. (N.Y.)* **1975**, *1*, 5–9.
(12) Dobry-Duclaux, A.; Perichon, P. *J. Chim. Phys. Phys.-Chim. Biol.* **1976**, *73*, 1058.
(13) Sugiura, Y. *Inorg. Chem.* **1978**, *17*, 2176.
(14) Sugiura, Y.; Hirayama, Y. *J. Am. Chem. Soc.* **1977**, *99*, 1581.
(15) Sugiura, Y.; Hirayama, Y. *Inorg. Chem.* **1976**, *15*, 679.
(16) Sugiura, Y.; Hirayama, Y.; Tanaka, H.; Ishizu, K. *J. Am. Chem. Soc.* **1975**, *97*, 5577.
(17) Kroneck, P.; Naumann, C.; Hemmerich, P. *Inorg. Nucl. Chem. Lett.* **1971**, *7*, 659.
(18) Livingstone, S. E.; Oluka, J. E. *Transition Met. Chem. (N.Y.)* **1977**, *2*, 163–168.
(19) Livingstone, S. E.; Oluka, J. E. *Transition Met. Chem. (N.Y.)* **1977**, *2*, 190–194.
(20) MacDonald, L.; Brown, D. H.; Smith, W. E. *Inorg. Chim. Acta* **1979**, *33*, L183.
(21) Sakurai, H.; Yokoyama, A.; Tanaka, H. *Chem. Pharm. Bull.* **1970**, *18*, 2373.
(22) Birker, P. J. M. W. L.; Freeman, H. C. *J. Am. Chem. Soc.* **1977**, *99*, 6890.
(23) Birker, P. J. M. W. L. *Inorg. Chem.* **1979**, *18*, 3502.
(24) Schugar, H. J.; Ou, C.; Thich, J. A.; Potenza, J. A.; Felthouse, T. R.; Haddad, M. S.; Hendrickson, D. N.; Furey, W.; Lalancette, R. A. *Inorg. Chem.* **1980**, *19*, 543–552.
(25) Hughey, J. L.; Fawcett, T. G.; Rudich, S. M.; Lalancette, R. A.; Potenza, J. A.; Schugar, H. J. *J. Am. Chem. Soc.* **1979**, *101*, 2617.
(26) Lappin, A. G.; McAuley, A. *J. Chem. Soc., Dalton Trans.* **1978**, 1606–1609.

0020-1669/83/1322-1267$01.50/0

redox reaction was initiated by attack on this dimeric two-electron reduction template by the sulfhydryl group of a noncoordinated molecule of 2-mercaptosuccinic acid. Assuming that this nonradical process is indeed the normal kinetic pathway to the undesirable redox products (i.e., copper(I) and the disulfide), we have incorporated in our initial synthetic schemes several features designed to slow down or eliminate the dimerization and rate-determining steps of this mechanism.

Specifically, we invariably bind the copper(II) ion with a macrocyclic or polydentate ligand before introduction of the thiol to the synthetic mixture. The extremely stable and relatively inert complexes thus formed shift the redox potential of the bound metal (making it more difficult to reduce) and block all coordination sites except the site to be used by the thiolate ligand, thus preventing the dimerization step. One of the best ligands for this purpose is the monoanion **1** of

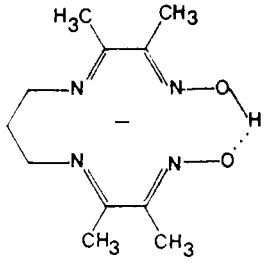

1

4,8-diaza-3,9-dimethylundeca-3,8-diene-2,10-dione dioxime, which we have called "Pre-H" (due to its status as a synthetic precursor to the macrocyclic cyclops ligand) in earlier studies.[27] In addition to the use of these "stabilizing" ligands, we have chosen in our initial studies to use thiophenols as our thiol-bearing ligands, due to the lower oxidation potentials of these species relative to aliphatic thiols. Low temperature has been employed to slow further the steps of the redox process. Careful control of the reaction stoichiometry is necessary to keep the concentration of unbound thiol (which initiates the redox process; see above) as low as possible.

Utilizing this synthetic scheme, we have observed a variety of aromatic and aliphatic thiols to form intensely colored complexes when allowed to react with the copper(II) complex of ligand **1** above. The synthesis and properties of two such copper(II)–mercaptide complexes, (*p*-chlorothiophenolato)-(3,9-dimethyl-4,8-diazaundeca-3,8-diene-2,10-dione dioximato)copper(II) ([Cu(**1**)(*p*-ClC_6H_4S)] (**2**)) and (thiophenolato)(3,9-dimethyl-4,8-diazaundeca-3,8-diene-2,10-dione dioximato)copper(II)([Cu(**1**)(C_6H_5S)] (**3**)), are the subject of this report.

Experimental Section

Synthesis. (a) [Cu(1)(*p*-ClC_6H_4S)] (2). *p*-Chlorothiophenol (0.184 g, 1.27 mmol) was added to a degassed solution of potassium hydroxide in methanol (40.0 mL, 0.032 M, 1.27 mmol). The resultant solution of the *p*-$ClC_6H_4S^-$ anion was cooled (ice bath) and added dropwise, under argon, to a stirred, cooled (ice bath) solution [Cu(**1**)-(OH_2)]$ClO_4 \cdot H_2O$ (prepared as in ref 27) in methanol (20.0 mL, 0.058 M, 1.16 mmol). During this addition, the initial brownish red solution of the aquo complex turned intensely dark green. This dark green solution was refrigerated at −15 °C for 12 h, and the solid product was then isolated by filtration, washed with cold water to remove the $KClO_4$ impurity, and dried in air. The final yield of **2** was 0.37 g (71%) by this method. Anal. Calcd for $C_{17}H_{23}N_4O_2CuSCl$: C, 45.73; H, 5.19; N, 12.55. Found: C, 45.23; H, 5.2; N, 12.07 (Huffman Laboratories, Wheat Ridge, CO). IR bands (cm^{-1}, with assignments): 454 m, 497 m, 528 m, 542 m, 686 m, 795 m, 816 s, 842 m, 982 m, 1010 s, 1087 vs, 1093 vs (Cl–C(aromatic) stretch), 1127 s, 1224 m, 1328 m, 1532 m and 1608 m (imine stretching modes, assigned similarly to ref 28), 3028 w.

(27) Anderson, O. P.; Packard, A. B. *Inorg. Chem.* **1979**, *18*, 1940–1947.
(28) Eggleston, D. S.; Jackels, S. C. *Inorg. Chem.* **1980**, *19*, 1593–1599.

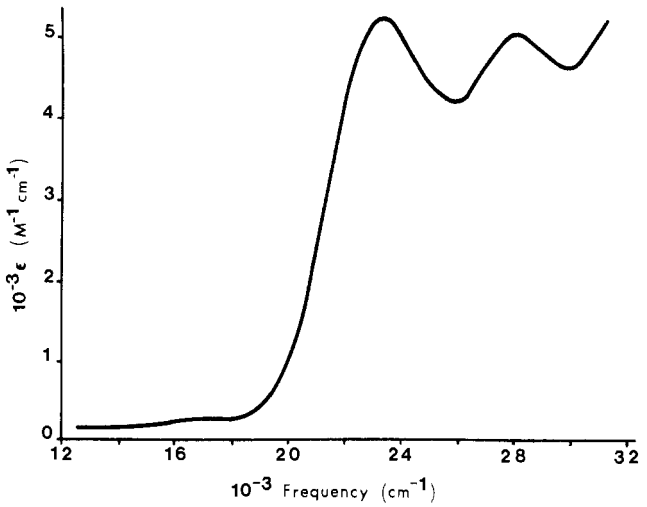

Figure 1. Visible spectrum of copper(II)–mercaptide complex **3** in CH_2Cl_2.

(b) [Cu(1)(C_6H_5S)] (3). Thiophenol (1.00×10^{-1} mL, 1.00 mmol) was added, under argon, to a solution of lithium hydroxide in methanol (20.0 mL, 0.050 M, 1.00 mmol). The resultant solution of the $C_6H_5S^-$ anion was cooled (ice bath) and added dropwise, under argon, to a stirred, cooled (ice bath) solution of [Cu(**1**)(OH_2)]PF_6 (see below) in acetone (20.0 mL, 0.050 M, 1.00 mmol). Approximately 25 mL of solvent was removed under vacuum, and the resultant dark green, cold solution was refrigerated at −30 °C for 12 h. The extremely dark crystalline product was isolated by filtration, washed with cold water, and dried in air; yield 0.186 g (45.2%). Anal. Calcd. for $C_{17}H_{24}N_4O_2CuS$: C, 49.56; H, 5.87; N, 13.60. Found: C, 49.97; H, 6.0; N, 13.35 (Huffman Laboratories, Wheat Ridge, CO). IR bands (cm^{-1}, with some assignments): 454 m, 658 w, 685 m, 696 vs, 744 vs, 792 m, 840 m, 1012 m, 1022 s, 1055 m, 1082 s, 1122 sh, 1124 s, 1328 m, 1417 m, 1538 m and 1606 m (imine symmetric and antisymmetric stretching modes[28]), 1572 s, 3056 w.

(c) [Cu(1)(OH_2)](BF_4) (4). This material, which was used in the electrochemical experiments (see below), was synthesized as follows. Copper(II) acetate monohydrate (1.00 g, 5.0 mmol) and HBF_4 (0.91 mL of 48% solution in water, 5.0 mmol) were added to 10 mL of water, and the solution was stirred until the solid dissolved. The resultant blue solution was added dropwise to a stirred solution of **1** (1.20 g, 5.0 mmol) in 10 mL of methanol. The brown crystals obtained on partial evaporation of the methanol were isolated by filtration and dried in air; yield 1.49 g (73%). Imine stretching bands were observed in the IR spectrum at 1629 and 1539 cm^{-1}, and bands at 3580 and 3500 cm^{-1} were attributed to bound water.

(d) [Cu(1)(OH_2)]PF_6. This salt, used in the synthesis of **3** (see above), was prepared from the corresponding perchlorate salt. [Cu(**1**)(OH_2)]$ClO_4 \cdot H_2O$ (0.75 g, 1.82 mmol) was dissolved in 10 mL of a 50:50 mixture (by volume) of methanol and water. A solution of ammonium hexafluorophosphate (0.30 g, 1.82 mmol) in 10 mL of water was added dropwise to the stirred solution containing the perchlorate salt. The brown crystalline product that formed was isolated by filtration and dried in air; yield 0.53 g (62.5%).

Visible Spectra. Due to the ready decomposition of solutions of compounds **2** and **3** when exposed to oxygen and the thermal instability of solutions at room temperature, the following procedure was adopted for determination of the visible spectroscopic parameters reported below. A preweighed sample of the solid was added to a tared flask, which possessed a side arm that terminated in a 2-mm silica cell. On the vacuum line, methylene chloride was distilled into the flask, and the resultant solution was sealed under vacuum. Weighing of the assembly at this point allowed calculation of the concentration of the solution.

While cooled solutions of **2** and **3** were stable indefinitely, these room-temperature solutions used for the visible spectra decomposed slowly ($t_{1/2}$ on the order of several hours). To determine the absorbance of the original solution, spectra were taken at frequent intervals for 3 h, and a final spectrum was taken after approximately 24 h, when no further change in the spectrum was occurring. Since the measurements taken during the initial period seemed to obey first-order kinetics, plots of ln $(A - A_\infty)$ for the peak absorbances were ex-

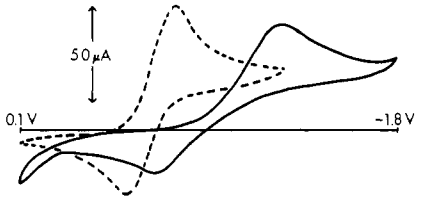

Figure 2. Cyclic voltammograms of copper(II)–mercaptide complex **2** (solid line) and aquo complex **4** (dashed line) in CH_2Cl_2 at 0 °C (scan rate 100 mV s^{-1}).

trapolated to give values for A_0, from which the extinction coefficients reported below were determined. Figure 1 shows the visible spectrum obtained for compound **3** 15 min after its initial dissolution.

Magnetic Susceptibility. The magnetic susceptibilities of **2** and **3** were determined at room temperature with a Cahn 7600 Faraday balance ($Hg[Co(NCS)_4]$ calibrant).

Electrochemistry. Cyclic voltammetric measurements were carried out in the laboratory of Professor C. M. Elliott, Colorado State University. Methylene chloride (Aldrich) was used as solvent after purification by passage over alumina and distillation from calcium hydride. Tetra-*n*-butylammonium perchlorate (Eastman) was used as supporting electrolyte in all cases.

Cooled (ice bath) solutions (5×10^{-3} M) of **2**, **3**, **4**, and freshly sublimed ferrocene in degassed CH_2Cl_2 were transferred to the nitrogen-flushed electrochemical cell, which was maintained at ice-bath temperature throughout each experiment. The electrode configuration employed included a glassy-carbon working electrode, a platinum auxiliary electrode, and a saturated calomel reference electrode. The actual measurements were performed with a PAR 173 potentiostat/galvanostat in conjunction with a PAR 175 universal programmer and a PAR 179 digital coulometer. Tracings of typical scans for **2** and **4** at 100 mV s^{-1} are shown in Figure 2.

X-ray Structure Determination. (a) For a dark green crystal of [Cu(**1**)(*p*-ClC_6H_4S)] (**2**) ($C_{17}H_{23}N_4O_2CuSCl$, formula weight 446.46), Weissenberg and precession photographs revealed only Laue symmetry $2/m$, together with systematic absences for $h0l$ ($l = 2n + 1$) and $0k0$ ($k = 2n + 1$), which allowed assignment of $P2_1/c$ (No. 14) as the space group.[29] The crystal was carefully centered on the Nicolet R3 diffractometer, and the setting angles for 23 reflections (2θ(av) = 18.45°, Mo Kα radiation with graphite monochromator, λ = 0.710 73 Å) allowed least-squares calculation[30] of the following cell constants: a = 10.536 (2) Å, b = 12.793 (3) Å, c = 15.061 (3) Å, β = 105.50 (1)°, and V = 1956.2 Å^3. With Z = 4, ρ(calcd) = 1.52 g cm^{-3}.

The intensities of all reflections for which $3.5° < 2\theta < 50.0°$, $h \geq 0$, and $k \geq 0$ were measured by using θ–2θ scans, a scan range of $[2.1 + 1.0(2\theta_{K\alpha_1} - 2\theta_{K\alpha_2})]°$, variable scan speed (2.02–29.30° min^{-1}), and background measurements at the scan extremes (taken for half the total scan time). The intensities of three control reflections (131, 027, and 41$\bar{6}$), monitored every 100 reflections, showed no significant trend during the course of data collection. No absorption correction was carried out, due to the low absorption coefficient (μ = 13.8 cm^{-1}) and the small size of the crystal, which was bounded by {001}, {011}, {110}, and {1$\bar{1}$0} and had approximate dimensions of 0.06 mm × 0.12 mm × 0.34 mm. Lorentz and polarization corrections were carried out, and 2294 unique reflections (of 3079 total) were taken to be observed ($I > 2.5\sigma(I)$) and were used in least-squares refinement.

The structure was solved by the direct-methods routine SOLV[30] and refined by using anisotropic thermal parameters for all non-hydrogen atoms. Neutral-atom scattering factors (including anomalous scattering) were taken from ref 31. Most hydrogen atoms were included in calculated positions 0.96 Å from carbon, with isotropic thermal parameters 1.2 times the equivalent isotropic value for the heavier atom. The only exception was the hydrogen atom (H18) involved in hydrogen bonding between the oxime oxygen atoms O1 and O2. This atom was located as the highest peak in a difference Fourier map late in the refinement and was subsequently refined with an isotropic thermal parameter. The refinement program in the SHELXTL package[30] carries out refinement in large blocks (maximum number of parameters per block is 103) rather than full matrix, and thus a complete pass through the 252 adjustable parameters for this structure requires three such blocked least-squares cycles. Weighted least-squares refinement (data:parameter ratio 9.1), with weights calculated as $\{\sigma^2(R) + gF^2\}^{-1}$ and $g = 3.9 \times 10^{-4}$ (final refined value), to convergence (average shift/esd < 0.10 over last six cycles) resulted in R = 0.041, R_w =

Table I. Fractional Atomic Coordinates (×10^4)[a] for [Cu(**1**)(*p*-ClC_6H_4S)]

atom	*x*	*y*	*z*
Cu	−1172 (1)	1122 (1)	3357 (1)
S	−2344 (1)	2746 (1)	2883 (1)
Cl	−5950 (1)	3014 (1)	5604 (1)
N1	−299 (3)	1468 (3)	4665 (2)
N2	−2374 (3)	426 (3)	3987 (2)
N3	−1559 (3)	194 (3)	2278 (2)
N4	449 (3)	1318 (2)	2969 (2)
O1	824 (3)	2047 (2)	4945 (2)
O2	1426 (3)	1929 (2)	3426 (2)
C1	−945 (4)	1270 (3)	5250 (3)
C2	−2155 (4)	635 (3)	4845 (3)
C3	−3511 (4)	−202 (4)	3490 (3)
C4	−3793 (4)	−56 (4)	2449 (3)
C5	−2752 (4)	−450 (4)	2016 (3)
C6	−663 (4)	171 (3)	1847 (3)
C7	518 (4)	826 (3)	2229 (3)
C8	−537 (5)	1623 (4)	6226 (3)
C9	−3003 (5)	311 (4)	5454 (3)
C10	−715 (5)	−494 (4)	1020 (3)
C11	1679 (5)	880 (4)	1842 (3)
C12	−3337 (4)	2810 (3)	3653 (3)
C13	−4638 (4)	2447 (3)	3412 (3)
C14	−5418 (4)	2491 (3)	4006 (3)
C15	−4923 (4)	2910 (3)	4871 (3)
C16	−3647 (4)	3263 (4)	5144 (3)
C17	−2870 (4)	3209 (3)	4539 (3)
H18[b]	1114 (37)	2108 (31)	4380 (27)

[a] Estimated standard deviations in the least significant digits are given in parentheses. [b] Isotropic U for this atom is 0.06 (1) Å^2.

Table II. Atom Coordinates (×10^4)[a] for [Cu(**1**)(C_6H_5S)]

atom	*x*	*y*	*z*
Cu	3854 (1)	6442 (1)	670 (1)
S	2276 (1)	6629 (1)	1332 (1)
N1	3642 (2)	7163 (2)	−197 (1)
N2	4803 (2)	7441 (2)	873 (1)
N3	4573 (2)	5563 (2)	1280 (1)
N4	3522 (2)	5306 (1)	169 (1)
O1	3031 (2)	6911 (1)	−720 (1)
O2	2940 (2)	5259 (1)	−430 (1)
C1	4166 (2)	7896 (2)	−238 (2)
C2	4840 (2)	8041 (2)	385 (2)
C3	5457 (2)	7468 (2)	1505 (2)
C4	5113 (3)	6809 (2)	2059 (2)
C5	5213 (2)	5829 (2)	1878 (2)
C6	4385 (2)	4737 (2)	1136 (1)
C7	3750 (2)	4575 (2)	493 (1)
C8	4118 (3)	8500 (2)	−872 (2)
C9	5530 (3)	8834 (2)	402 (2)
C10	4752 (3)	3954 (2)	1558 (2)
C11	3418 (3)	3674 (2)	252 (2)
C12	2269 (2)	5615 (2)	1803 (1)
C13	1860 (2)	4834 (2)	1518 (2)
C14	1887 (2)	4031 (2)	1881 (2)
C15	2320 (2)	3983 (2)	2545 (2)
C16	2711 (2)	4741 (2)	2844 (2)
C17	2684 (2)	5554 (2)	2481 (2)
H18[b]	2917 (27)	5908 (22)	−598 (16)

[a] Estimated standard deviations in the least significant digits are given in parentheses. [b] Isotropic U for this atom equals 0.08 (1) Å^2.

(29) "International Tables for X-Ray Crystallography"; Kynoch Press: Birmingham, England, 1969; Vol. I.
(30) Programs used in initial centering and data collection were supplied with the Nicolet R3 diffractometer. Programs used in structure solution, refinement, and plotting were part of the SHELXTL program package written by G. M. Sheldrick and supplied by Nicolet XRD for the Data General Eclipse S/140 computer in this laboratory.
(31) "International Tables for X-Ray Crystallography"; Kynoch Press: Birmingham, England, 1969; Vol. IV, pp 55, 99, 149.

Table III. Bond Lengths (Å) and Angles (deg) for [Cu(**1**)(*p*-ClC$_6$H$_4$S)][a]

Cu-S	2.424 (1)	Cu-N1	1.988 (3)
Cu-N2	1.985 (4)	Cu-N3	1.965 (3)
Cu-N4	1.964 (4)	S-C12	1.759 (5)
Cl-C15	1.746 (5)	N1-O1	1.364 (4)
N1-C1	1.275 (6)	N2-C2	1.279 (6)
N2-C3	1.470 (5)	N3-C5	1.467 (5)
N3-C6	1.281 (6)	N4-O2	1.328 (4)
N4-C7	1.299 (5)	C1-C2	1.498 (5)
C1-C8	1.487 (6)	C2-C9	1.499 (7)
C3-C4	1.527 (7)	C4-C5	1.505 (7)
C6-C7	1.483 (5)	C6-C10	1.497 (6)
C7-C11	1.491 (7)	C12-C13	1.401 (5)
C12-C17	1.389 (6)	C13-C14	1.369 (7)
C14-C15	1.375 (6)	C15-C16	1.373 (6)
C16-C17	1.381 (7)		
S-Cu-N1	99.5 (1)	S-Cu-N2	100.6 (1)
N1-Cu-N2	79.1 (1)	S-Cu-N3	107.3 (1)
N1-Cu-N3	153.2 (1)	N2-Cu-N3	96.1 (1)
S-Cu-N4	102.6 (1)	N1-Cu-N4	93.3 (1)
N2-Cu-N4	156.4 (1)	N3-Cu-N4	80.5 (1)
Cu-S-C12	101.1 (1)	Cu-N1-O1	124.1 (3)
Cu-N1-C1	116.8 (3)	O1-N1-C1	118.2 (3)
Cu-N2-C2	115.1 (3)	Cu-N2-C3	122.6 (3)
C2-N2-C3	122.1 (4)	Cu-N3-C5	122.4 (3)
Cu-N3-C6	114.5 (3)	C5-N3-C6	123.0 (3)
Cu-N4-O2	122.4 (3)	Cu-N4-C7	116.5 (3)
O2-N4-C7	121.1 (4)	N1-C1-C2	112.3 (3)
N1-C1-C8	123.8 (4)	C2-C1-C8	123.8 (4)
N2-C2-C1	115.4 (4)	N2-C2-C9	125.7 (4)
C1-C2-C9	118.9 (4)	N2-C3-C4	111.4 (4)
C3-C4-C5	116.1 (4)	N3-C5-C4	111.5 (4)
N3-C6-C7	116.5 (4)	N3-C6-C10	124.5 (4)
C7-C6-C10	119.0 (4)	N4-C7-C6	111.9 (4)
N4-C7-C11	123.6 (4)	C6-C7-C11	124.4 (4)
S-C12-C13	121.8 (3)	S-C12-C17	122.0 (3)
C13-C12-C17	116.2 (4)	C12-C13-C14	122.3 (4)
C13-C14-C15	119.5 (4)	Cl-C15-C14	119.1 (3)
Cl-C15-C16	120.5 (3)	C14-C15-C16	120.4 (4)
C15-C16-C17	119.4 (4)	C12-C17-C16	122.2 (4)

[a] Estimated standard deviations in the least significant digits are given in parentheses.

Table IV. Bond Lengths (Å) and Angles (deg)[a] for [Cu(**1**)(C$_6$H$_5$S)]

Cu-S	2.424 (1)	Cu-N1	1.971 (2)
Cu-N2	1.979 (2)	Cu-N3	1.981 (2)
Cu-N4	1.988 (2)	S-C12	1.756 (3)
N1-O1	1.321 (3)	N1-C1	1.294 (3)
N2-C2	1.282 (3)	N2-C3	1.465 (4)
N3-C5	1.456 (4)	N3-C6	1.286 (3)
N4-O2	1.362 (3)	N4-C7	1.285 (3)
C1-C2	1.481 (4)	C1-C8	1.496 (4)
C2-C9	1.491 (4)	C3-C4	1.500 (4)
C4-C5	1.509 (4)	C6-C7	1.485 (4)
C6-C10	1.492 (4)	C7-C11	1.486 (4)
C12-C13	1.390 (4)	C12-C17	1.387 (4)
C13-C14	1.381 (4)	C14-C15	1.372 (5)
C15-C16	1.364 (5)	C16-C17	1.394 (5)
S-Cu-N1	104.0 (1)	S-Cu-N2	110.3 (1)
N1-Cu-N2	80.5 (1)	S-Cu-N3	100.6 (1)
N1-Cu-N3	155.1 (1)	N2-Cu-N3	95.2 (1)
S-Cu-N4	99.0 (1)	N1-Cu-N4	92.6 (1)
N2-Cu-N4	150.7 (1)	N3-Cu-N4	79.1 (1)
Cu-S-C12	99.4 (1)	Cu-N1-O1	122.9 (2)
Cu-N1-C1	116.0 (2)	O1-N1-C1	121.1 (2)
Cu-N2-C2	114.4 (2)	Cu-N2-C3	122.9 (2)
C2-N2-C3	122.6 (2)	Cu-N3-C5	122.6 (2)
Cu-N3-C6	115.0 (2)	C5-N3-C6	122.2 (2)
Cu-N4-O2	123.9 (2)	Cu-N4-C7	116.8 (2)
O2-N4-C7	118.5 (2)	N1-C1-C2	113.0 (2)
N1-C1-C8	122.5 (3)	C2-C1-C8	124.5 (3)
N2-C2-C1	116.1 (2)	N2-C2-C9	124.3 (3)
C1-C2-C9	119.6 (3)	N2-C3-C4	111.7 (2)
C3-C4-C5	117.1 (3)	N3-C5-C4	112.8 (2)
N3-C6-C7	115.7 (2)	N3-C6-C10	125.4 (2)
C7-C6-C10	118.9 (2)	N4-C7-C6	112.1 (2)
N4-C7-C11	123.9 (2)	C6-C7-C11	124.0 (2)
S-C12-C13	122.1 (2)	S-C12-C17	121.2 (2)
C13-C12-C17	116.7 (3)	C12-C13-C14	122.0 (3)
C13-C14-C15	120.3 (3)	C14-C15-C16	119.1 (3)
C15-C16-C17	120.8 (3)	C12-C17-C16	121.1 (3)

[a] Estimated standard deviations in the least significant digits are given in parentheses.

0.0397, and the error in an observation of unit weight equal to 1.321. In a final ΔF synthesis, the two highest peaks were 0.9 Å from Cl (0.43 e Å^{-3}) and 0.88 Å from S (0.37 e Å^{-3}). Analysis of variance as a function of Bragg angle, magnitude of F, reflection indices, etc. showed no strong trends. A normal probability plot[32] at this point exhibited a slope of 1.174.

The final atomic coordinates for **2** are contained in Table I, and bond lengths and angles derived from these coordinates are found in Table III. The following tables have been supplied as supplementary material: Table VI, least-squares planes for **2**; Table VIII, a listing of the anisotropic thermal parameters for **2**; Table X, the calculated hydrogen atom coordinates and thermal parameters for **2**; Table XII, a listing of $10F_o$ and $10F_c$ for the reflections comprising the data set for **2**.

(b) A dark green crystal of [Cu(**1**)(C$_6$H$_5$S)] (**3**) (formula C$_{17}$H$_{24}$N$_4$O$_2$CuS, formula weight 412.01) was centered on the Nicolet R3 diffractometer. Least-squares treatment of 25 reflections for which $20° < 2\theta < 25°$ (Mo Kα radiation with graphite monochromator, λ = 0.71073 Å) yielded an orthorhombic cell with a = 13.072 (2) Å, b = 14.940 (2) Å, c = 18.786 (3) Å. and V = 3668.9 Å^3. The crystal density was determined to be 1.47 g cm^{-3} by neutral buoyancy in a mixture of 1,2-dibromoethane and benzene; this value compares well with ρ(calcd) of 1.49 g cm^{-3} for Z = 8. Axial photos taken on the Nicolet R3 diffractometer about a, b, and c verified the required *mmm* Laue symmetry for the orthorhombic system.

Data collection, structure solution, and least-squares refinement were carried out in a manner similar to that for **2**, and only points of difference will be mentioned here. Intensities of all reflections for which $4° < 2\theta < 50°$, $h \geq 0$, $k \geq 0$, and $l \geq 0$ were collected. Intensities of three control reflections (0,0,10, 721, and 275) were monitored every 200 reflections, and no significant trend in these intensities was apparent during data collection.

An empirical absorption correction, based on intensity profiles for 15 reflections over a range of setting (ψ) for the diffraction vector, was applied to the observed data. The crystal measured roughly 0.22 mm × 0.23 mm × 0.44 mm and was bounded by {10$\bar{1}$}, {101}, and {0$\bar{1}$0}. With μ = 13.19 cm^{-1}, the applied transmission factors ranged ±5% about the mean value.

Systematic extinctions ($0kl$, $k = 2n + 1$; $h0l$, $l = 2n + 1$; $hk0$, $h = 2n + 1$) observed in the resultant data set required assignment of *Pbca* (No. 61)[29] as the space group. Least-squares refinement of 243 parameters was carried to convergence for the 2572 unique, observed reflections (a total of 3072 intensities were measured), resulting in R = 0.030, R_w = 0.033, and the standard deviation in an observation of unit weight of 1.631. The parameter g in the weighting scheme (see above) refined to 2.8 × 10^{-4}, and an adjustable isotropic secondary extinction parameter[33] refined to 1.7 (4) × 10^{-3}. The highest peak in the final ΔF map was 0.31 e Å^{-3} in the vicinity of C3 and C4. The final normal probability plot gave a slope of 1.341.

The final atomic coordinates for **3** may be found in Table II, while bond lengths and angles for **3** are in Table IV. Supplementary material provided includes the following tables: Table VII, least-squares planes for **3**; Table IX, anisotropic thermal parameters for **3**; Table XI, calculated hydrogen atom positions and isotropic thermal parameters for **3**; Table XIII, a listing of $10F_o$ and $10F_c$ for the reflections used in refinement.

Results and Discussion

Initial observations on complexes **2** and **3** strongly supported the presence of a Cu(II)–S(mercaptide) bond in both cases. Both compounds were found to be paramagnetic to an extent

(32) Abrahams, R. *Acta Crystallogr., Sect. B* **1974**, *B30*, 261–268.

(33) Larson, A. C. *Acta Crystallogr.* **1967**, *23*, 664.

normal for monomeric copper(II) complexes, with μ_{eff} (corrected for diamagnetism) equal to 2.0 μ_B for **2** and 1.8 μ_B for **3**. The visible spectra were very similar for the two complexes, with **2** exhibiting two intense transitions at 428 (23 400 cm^{-1}, ϵ = 5310 M^{-1} cm^{-1}) and 354 nm (28 200 cm^{-1}, ϵ = 5325 M^{-1} cm^{-1}). A spectrum obtained for **3** before significant decomposition had taken place (see above) is shown in Figure 1, and the two prominent bands seen in this spectrum occur at 428 nm (ϵ = 5490 M^{-1} cm^{-1}) and 355 nm (ϵ = 5200 M^{-1} cm^{-1}). There can be no doubt that these bands are a result of copper(II)–S(mercaptide) binding, since the thiolate anions used are essentially colorless and the parent complex (**4**) exhibits only a weak shoulder at 480 nm (ϵ = 343 M^{-1} cm^{-1}) on an extremely intense peak that has its maximum somewhere below 330 nm. This latter band for **4**, which is presumably due to charge transfer between ligand **1** and the copper atom, would also account for the high absorption above the peak at 28 100 cm^{-1} in Figure 1.

It is tempting, for several reasons, to assign the two bands reported above for **2** and **3** to the σ and π LMCT (ligand-to-metal charge transfer) processes responsible for the intense transitions characteristic of the "blue" copper proteins.[34] First, the bands seen in **2** and **3** are very similar in energy to the bands seen for [Cu(tet b)(*o*-mercaptobenzoate)] (λ = 425, 360 nm), which were assigned as σ and π LMCT bands,[25] although the intensities of the bands for **2** and **3** are 3–5 times higher than those for the mercaptobenzoate complex. Also, the separation of 4800 cm^{-1} between the two prominent bands of **2** and **3** is at one extreme of the range of 3800–4800 cm^{-1} characteristic of the energy differences between the charge-transfer bands of the "blue" copper proteins.[34] The blue shift of approximately 11 000 cm^{-1} for the bands of **2** and **3** relative to the corresponding bands for the proteins reflects the shifts in redox potential of the Cu(II)/Cu(I) couple and the thiolate ligands in **2** and **3** relative to the proteins. In fact, as will be seen in the electrochemical discussion below, the difference between the potentials exhibited by **2** and **3** and the potentials characteristic of the type 1 copper centers in proteins shows a stabilization of **2** and **3** relative to the proteins that matches very closely the blue shift seen in these spectra.

The copper–sulfur binding inferred from the spectra of **2** and **3** has been confirmed by a determination of the structures of these complexes. While we had originally supposed that the *p*-chloro substituent on the thiophenol ligand would alter to some significant degree the properties of the mercaptide complexes, the similarity in spectra for **2** and **3** belies that assumption and suggests that the structures of **2** and **3** should be very similar. In fact, the structures (see Figure 3) are close in all respects and will be discussed together in the following paragraphs.

Both **2** and **3** occur as discrete, neutral, monomeric square-pyramidal complexes, with the mercaptide sulfur atom occupying the apical position and the nitrogen atoms of ligand **1** occupying the basal positions. Packing diagrams (Figure 4) suggest that no chemically significant intermolecular interactions occur, and this has been verified by calculation of all possible contacts for copper and sulfur out to a distance of 3.5 Å for both atoms. Thus, despite the known propensity of mercaptide sulfur to bridge between two metals, the strongly coordinating ligand **1** apparently blocks this mode of binding in these complexes, as was anticipated above.

The copper–sulfur distance (2.424 (1) Å in both **2** and **3**) is only slightly longer than the value of 2.359 (4) Å observed

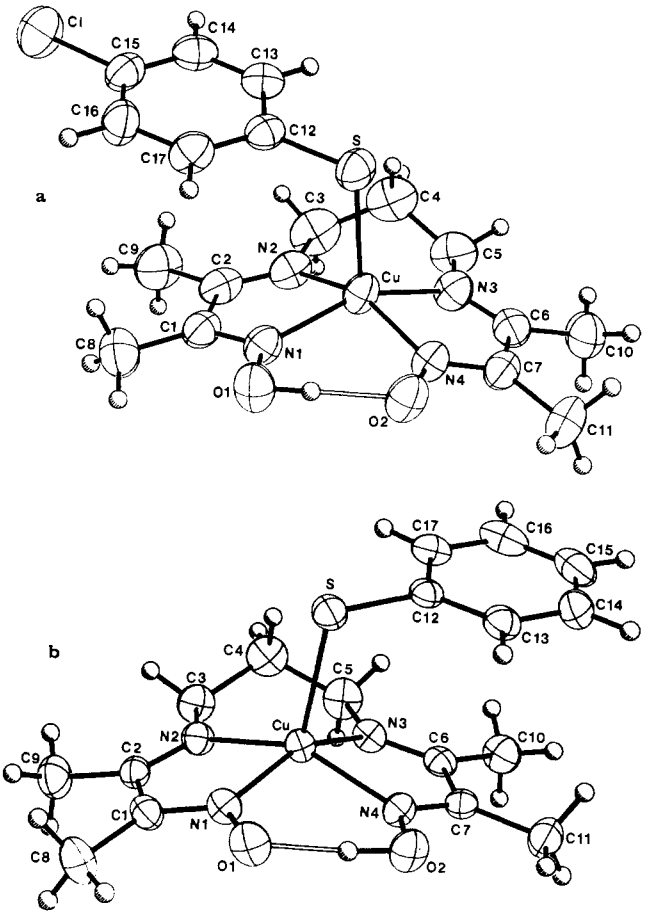

Figure 3. (a) Structure of the Cu(II)–*p*-chlorothiophenol complex, **2**, showing the numbering scheme. Thermal ellipsoids have been drawn at the 50% probability level for non-hydrogen atoms. Hydrogen atoms have been included with fixed, arbitrary radius. (b) Structure of the Cu(II)–thiophenol complex, **3**.

for [Cu(tet b)(*o*-mercaptobenzoate)].[25] In that complex, the sulfur atom was bound to one of the equatorial sites of a trigonal-bipyramidal (tbp) ligand array. Since bonds to copper(II) at equatorial tbp positions are generally strong, the small difference between the Cu–S bond lengths in **2** and **3** and that for the *o*-mercaptobenzoate adduct suggests that the Cu(II)–S(mercaptide) bonding in **2** and **3** is stronger than would normally be expected for a ligand in an apical square-pyramidal site. Similar strong apical bonding has been seen in other square-pyramidal complexes in which anionic ligands occupied the apical coordination position.[35-37] However, the Cu–S bond lengths seen for **2**, **3**, and the mercaptobenzoate complex are all approximately 0.3 Å longer than the Cu–S bond length established by EXAFS studies for the "blue" copper site.[5] The angles observed at sulfur (101.1 (1)° for **2**, 99.4 (1)° for **3**) are similar to the value of 107° observed for plastocyanin[38] and the value of 108.4 (4)° seen for [Cu(tet b)(*o*-mercaptobenzoate)].[25] The lower values of this angle seen for **2** and **3** may well be the result of packing forces, as the copper–S–C12 angle should be quite susceptible to distortion by such means.

Other aspects of the observed structures of **2** and **3** suggest that the binding to apical sulfur is relatively strong. The copper–nitrogen bond lengths are significantly longer than those found in the aquo complex [Cu(**1**)(OH_2)]ClO_4·H_2O[27] (hereafter compound **5**) from which the mercaptide complexes **2** and **3** have been made. In **5**, no significant difference in Cu–N(imine) vs. Cu–N(oxime) bond lengths was seen, and

(34) Solomon, E. I.; Hare, J. W.; Gray, H. B. *Proc. Natl. Acad. Sci. U.S.A.* **1976**, *73*, 1389.
(35) Anderson, O. P.; Marshall, J. C. *Inorg. Chem.* **1978**, *17*, 1258.
(36) Anderson, O. P.; Packard, A. B. *Inorg. Chem.* **1979**, *18*, 3064.
(37) Anderson, O. P.; Packard, A. B. *Inorg. Chem.* **1980**, *19*, 2941.
(38) Reference 1f, p 27.

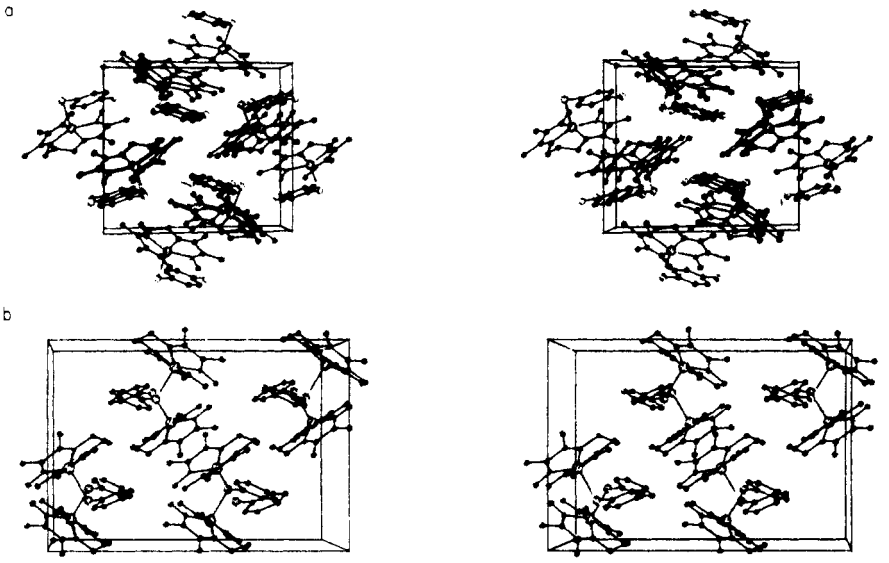

Figure 4. (a) Stereoview of the unit cell contents for **2**, viewed down *a*. (b) Stereoview of the structure of **3**, viewed down *b*.

Cu–N(av) was 1.957 (5) Å. In the mercaptide complexes **2** and **3**, average Cu–N distances are 1.976 (3) and 1.980 (2) Å, respectively. These significantly longer Cu–N distances for **2** and **3** are a consequence of the relatively strong apical mercaptide ligands pulling the metal atom out of the plane of the nitrogen atoms of ligand **1** (see below).

In passing, it should be noted that in neither of the complexes **2** and **3** is the expected Cu–N(imine) vs. Cu–N(oxime) bond length distinction observable. Instead, the distinction is between the N1–N2 ligand atom pair and the N3–N4 pair. It is most clear-cut in **2**, where Cu–N1 and Cu–N2 are equal at 1.988 (3) and 1.985 (4) Å, respectively, while Cu–N3 and Cu–N4 are also equal but distinctly shorter at 1.965 (3) and 1.964 (4) Å. In **3**, while Cu–N2 and Cu–N3 are equal at 1.979 (2) and 1.981 (2) Å, Cu–N1 and Cu–N4 are distinctly different at 1.971 (2) and 1.988 (2) Å. At first glance this difference would seem to depend on which side of the complex the phenyl ring of the mercaptide ligand is lying, but it is more likely to depend on the position of the hydrogen atom bridging the two oxime oxygen atoms. This atom (H18 in the coordinate list) was located, and its position was refined for both **2** and **3**. It appears from these results that the presence of H18 on O1 in **2** is associated with the longer Cu–N1 bond in that complex; the case is similar for O2 and Cu–N4 in **3**. The hydrogen bond between O1 and O2 is quite strong in both complexes. For **2**, O1–O2 = 2.537 (6) Å, H18–O1 = 0.98 (4) Å, and H18–O2 = 1.57 (5) Å, while for **3**, O1–O2 = 2.530 (4) Å, H18–O1 = 1.52 (4) Å, and H18–O2 = 1.02 (3) Å. While the O1–O2 distance in **5** (2.49 (1) Å) was shorter than either of these distances, the N1–N4 distance in **5** (2.91 (1) Å) was actually longer than observed in **2** or **3**, which may be related to further distortions in the ligand **1** in these complexes.

As mentioned above, one consequence of the relatively strong bond to apical sulfur in **2** and **3** is the large displacement of the copper(II) ion out of the plane of the four nitrogen atoms of ligand **1**. In both complexes, the nitrogen atoms are nearly coplanar, with a small tetrahedral distortion from a perfectly planar array (average displacement of N from the best least-squares plane for N1–N4 was 0.029 Å for **2** and 0.038 Å for **3**). The copper(II) atom is found 0.430 Å above this plane in **2** and 0.463 Å above it in **3**. These distances are striking, compared with the corresponding displacement of only 0.10 Å in **5**, where the much weaker aquo ligand occupied the apical position.

In **5**, where the metal was close to the four-nitrogen plane, the entire ligand **1** was nearly coplanar, with the exception of the central atom of the propylene moiety. However, the large out-of-plane displacement of copper seen in **2** and **3** forces a buckling of the ligand **1** to maintain effective orbital overlap between the nitrogen atoms and the copper. For example, the dihedral angles between the planes through the unsaturated sides (which remain highly planar throughout) of the complexes and the four-nitrogen reference plane are 7° (N1–N2 side) and 15° (N3–N4 side) for **2** and 18° (N1–N2 side) and 8° (N3–N4 side) for **3**. As was the case with the Cu–N bond lengths, the discrepancies between these dihedral angles and the distances by which copper is out of these planes through the unsaturated portions of the complex seem to correlate with the position of the hydrogen-bonding hydrogen atom H18. Thus, in **2** Cu is 0.26 Å above the N1–C1–C2–N2 plane but only 0.05 Å above the N3–C6–C7–N4 plane. In **3**, Cu is *in* the N1–C1–C2–N2 plane (displacement 0.00 Å) but 0.25 Å above the N3–C6–C7–N4 plane. The uneven buckling of the ligand **1** was only hinted at in complex **5**, where Cu was 0.10 Å out of the plane containing N1 and in the plane containing N4. Unfortunately, it is not possible to test the suggested correlation with H atom position with **5**, since the oxime hydrogen atom was not located in that study.

Other bond lengths and angles observed in the structures of **2** and **3** are much as expected from earlier studies. It is, perhaps, worth noting that the angles at sulfur allow the highly planar phenyl rings of the mercaptide ligands to lie nearly parallel to the four-nitrogen reference plane (dihedral angles of 12° in **2** and 8° in **3**).

The main features of these very similar structures—relatively strong Cu–S bonds and large out-of-plane copper displacements—affect the observed electrochemistry strongly. The cyclic voltammetric behavior seen in Figure 2 is typical of both mercaptide complexes, as can clearly be seen from the results in Table V. The reduction and oxidation waves shown for **2** in Figure 2 are the only waves in the cyclic voltammograms assignable to redox at the copper centers, since other waves were totally irreversible and were at the extremes of the scan range employed (approximately −2.0 V for an irreversible reduction and +0.4 V for an irreversible oxidation).

In Table V, the electrochemical results obtained for the mercaptide complexes **2** and **3** are compared with the potentials exhibited by the aquo complex **4** and ferrocene. Although all of these species exhibited cyclic voltammetric patterns under our temperature and concentration conditions which were (at best) quasi-reversible, the potential obtained for **4** agrees well with the $E_{1/2}$ of −0.56 V (vs. SHE in aqueous solution) obtained previously for the $[Cu(\mathbf{1})(OH_2)]^+$ complex cation[39] after

Table V. Electrochemistry of Copper(II) Mercaptides

compd	$E_{1/2}$, mV[a]	N[b]	ΔE_p, mV
[Cu(1)(*p*-ClC_6H_4S)] (**2**)	−860	0.88	668
[Cu(1)(C_6H_5S)] (**3**)	−850	0.80	616
[Cu(1)(OH_2)]BF_4 (**4**)	−490	0.85	265
ferrocene	500	1.00	376

[a] All results reported were obtained at a scan rate of 100 mV s^{-1} under the conditions described in the Experimental Section. $E_{1/2}$ values were calculated by taking $(E_{p,c} + E_{p,a})/2$. [b] Comparison of cathodic peak currents to that for ferrocene.

adjustment by the −0.100 V required to correct the ferrocene couple to the standard value of +0.400 V vs. the SHE. From the results shown, it appears clear that the binding of the mercaptide ligands is associated with a stabilization of the copper(II) state of approximately 350 mV. This stabilization must arise from the shift to the highly distorted five-coordinate geometry of **2** and **3**, compared to **4**. In addition, the greater donation of electron density to the metal by the more powerful mercaptide apical ligand should contribute to the observed shift in potential by making the copper(II) more difficult to reduce.

If the prominent bands observed in the visible spectra of **2** and **3** do indeed correspond to the σ(S)− and π(S)−Cu charge-transfer bands of the "blue" copper proteins, then the blue shift of ~11 000 cm^{-1} between the characteristic 600-nm band of the type 1 copper and the higher energy band at 354 nm for **2** should be seen again in the difference in electrochemical potentials for these species. Indeed, if one takes a typical potential for type 1 copper to be +400 mV vs. SHE, the 0.1-V correction cited above for our reference electrode would place type 1 copper at +500 mV in our system. The separation in potentials between our complexes **2** and **3** and the type 1 site would then be 1.35 V, which corresponds to 10 850 cm^{-1}. These electrochemical results thus provide further confirmation of the assignment of these intense visible transitions for **2** and **3** as LMCT transitions. More details of the orbitals involved in these transitions are expected to arise from our planned theoretical studies of the electronic structures of **2** and **3**.

Acknowledgment. We thank the Research Corp. (Grant No. 8076) and the National Institutes of Health (Grant No. GM 25302) for generous support of this work. Additional support from a Colorado State University Biomedical Research Support Grant (NIH Grant No. 534613) and the NATO Research Council (travel grant to O.P.A.) is also gratefully acknowledged. The Nicolet R3/E diffractometer and computer system were purchased with funds provided by the National Science Foundation (Grant No. CHE 8103011). The authors also wish to thank Dr. C. M. Elliott for helpful discussions and generous blocks of time on his electroanalytical instruments.

Registry No. **2**, 84927-41-3; **3**, 84927-42-4; **4**, 84927-43-5; [Cu(**1**)(OH_2)]ClO_4, 61114-06-5; [Cu(**1**)(OH_2)]PF_6, 84927-44-6.

Supplementary Material Available: Tables VI–XIII, showing least-squares planes, anisotropic temperature factors, positional parameters and isotropic temperature factors for hydrogen atoms, and structure factors for **2** and **3** (36 pages). Ordering information is given on any current masthead page.

(39) Gagnê, R. R.; Allison, J. L.; Gall, R. S.; Koval, C. A. *J. Am. Chem. Soc.* **1977**, *99*, 7170–7178.
(40) Bauer, D.; Breant, M. In "Electroanalytical Chemistry"; Bard, A. J., Ed.; Marcel Dekker: New York, 1975; Vol. VIII, p 306.

Contribution from the Departments of Chemistry, Radford University, Radford, Virginia 24142, and Virginia Polytechnic Institute and State University, Blacksburg, Virginia 24061

Interaction of Manganese(II) and Amino Acids with Emphasis on Cysteine and Penicillamine (β,β-Dimethylcysteine)

ROBERT K. BOGGESS,* JOHN R. ABSHER, SCOTT MORELEN, L. T. TAYLOR,* and JEFF W. HUGHES

Received August 31, 1982

The interaction of manganese(II) with bidentate and tridentate ligands containing nitrogen, oxygen, and/or sulfur donor atoms has been investigated. The tridentate amino acids L-cysteine and D-penicillamine have proven to be the best chelators for manganese(II) on the basis of aqueous titration data. Mono and bis chelates of high-spin manganese(II) employing these amino acids have been prepared and characterized. Oxygen-uptake experiments in solution have been carried out both on the isolated complexes and on prepared solutions of differing L:Mn(II):OH^- ratios. In each situation oxygen is rapidly consumed. Observations made during oxygenation experiments suggest that the sulfur-containing amino acid is oxidized to disulfide and that manganese catalyzes this reaction. An oxygenated manganese species is postulated as an intermediate with penicillamine.

Introduction

Reports of amino acid complexes with manganese(II) compared to those with other transition metal ions are less abundant partly due to their relatively weak interaction. For example, the formation constant (β_2) of the bis(L-histidinato)manganese(II) complex is some 6–12 orders of magnitude less than for other first-row transition-metal ions.[1] A recent review of amino acids with chelatable side-chain donor atoms[2] and two reviews specifically dealing with cysteine and penicillamine[3,4] rarely mention manganese(II) although chromium, iron, cobalt, nickel, copper, zinc, and several second- and third-row transition metals are discussed at length. A report specifically dealing with the chemistry of biological manganese devoted one short section to its interaction with amino acids.[5]

* To whom correspondence should be addressed: R.K.B., Radford University; L.T.T., Virginia Polytechnic Institute and State University.

(1) Martell, A. E.; Smith, R. M. "Critical Stability Constants"; Plenum Press: New York, 1974, 1975; Vols. 1 and 2.
(2) Martin, R. B. *Met. Ions Biol. Syst.* **1979**, *9*, Chapter 1.
(3) Gergely, A.; Sovago, I. *Met. Ions Biol. Syst.* **1979**, *9*, Chapter 3.
(4) McAuliffe, C. A.; Murray, S. G. *Inorg. Chim. Acta, Rev.* **1972**, 103.
(5) Lawrence, G. D.; Sawyer, D. T. *Coord. Chem. Rev.* **1978**, *27*, 173.

0020-1669/83/1322-1273$01.50/0